Polymer Degradation and Stability 249 (2026) 112080

Contents lists available at ScienceDirect

Polymer Degradation and Stability

journal homepage: www.journals.elsevier.com/polymer-degradation-and-stability

Long-term thermal aging of recycled polypropylene: Evaluation of different alditols, thiosynergists, and acid scavengers as novel stabilizer combinations

Kim Hao Ng, Katrin Markus, Jan-Hendrik Arndt, Elke Metzsch-Zilligen, Rudolf Pfaendner *

Research and Development, Fraunhofer Institute for Structural Durability and System Reliability LBF 64289, Darmstadt, Germany

ARTICLE INFO

Keywords:
Polypropylene
Long-term thermal aging
Mechanical recycling
Alditols
Acid scavengers
Thiosynergists
Stabilization

ABSTRACT

The long-term thermal stability of recycled polypropylene (rPP) is a critical factor for its use in durable applications and is strongly affected by oxidative degradation and stabilizer depletion during the previous life cycle. Novel stabilizer systems for rPP based on bio-derived components such as alditols or thiosynergists and inorganic acid scavengers were systematically investigated and compared to conventional and commercial recycle reference formulations. rPP from automotive battery cases was compounded with different additive combinations and subjected to accelerated oven aging at 150 °C and 135 °C. The aging behavior was evaluated using mechanical testing, melt volume rate measurements, determination of the carbonyl index, and molecular weight characterization through gel permeation chromatography. The results demonstrate that the choice of alditol, thiosynergist, and acid scavenger significantly influences the resistance to thermo-oxidative degradation. Several bio-based formulations show delayed embrittlement, reduced oxidation, and improved retention of molecular weight compared to standard phosphite-containing systems. The study highlights synergistic effects between stabilizer components, provides insight into structure-performance relationships relevant for the development of alternative stabilization strategies for rPP, and gives considerations of possible mechanisms of action for alditols.

1. Introduction

Among the major commodity plastics, polyolefins represent the largest share of global production due to their versatility, cost -efficiency, and broad application range [1]. Within this class, polypropylene (PP) is particularly important being widely used in packaging, automotive components, and durable goods [2]. With an annual production volume exceeding 80 million tons in 2024, PP accounts for a substantial share of global plastics demand [3]. According to current projections, the annual production could reach more than 130 million tons by 2034 [3]. Hence, its increasing consumption contributes significantly to the growing challenge of plastic waste [4,5]. This highlights the urgent need for stricter legislative recycling targets and in particular the need for effective recycling strategies in the context of the circular economy [6,7].

However, recycled (r) PP often exhibits inferior performance compared to virgin material [8]. This fact is primarily due to thermo-oxidative degradation which occurs during processing and service life leading to chain scission, loss of molecular weight, and embrittlement [9,10]. The degradation mechanism typically involves the formation of hydroperoxides resulting in the generation of carbonyl-containing species such as ketones, aldehydes, and acids [11–13]. These molecular changes translate into the respective macroscopic property losses [14]. Additional complications arise from the depletion of stabilizers during the first life cycle and the presence of contaminants which reduce the efficiency of conventional antioxidant systems [15,16]. To counteract these degradation pathways rPP requires the addition of suitable antioxidants that can restore stability and preserve material performance [8]. Therefore, the restabilization of recyclates has become an essential strategy to maintain processability and to extend service life in demanding long-term applications [8,17,18].

State-of-the-art long-term stabilization of polyolefins typically relies on combinations of sterically hindered phenols with thiosynergists such as distearyl 3,3'-thiodipropionate (DSTDP) or dilauryl 3,3'-thiodipropionate (DLTDP) [19]. These thioesters decompose hydroperoxides through a series of oxidation reactions forming inorganic sulfur-containing acids and sulfoxides which can further scavenge hydroperoxides, thereby providing effective long-term thermal stability mainly in the range of 100 to 150 °C [20]. Conventional stabilization strategies additionally employ combinations of sterically hindered phenols and organic phosphites which act as primary and secondary antioxidants [21,22]. Despite their effectiveness these systems face limitations in recycled streams and concerns have been raised about the health

* Corresponding author.
E-mail addresses: kim.hao.ng@lbf.fraunhofer.de (K.H. Ng), rudolf.pfaendner@lbf.fraunhofer.de (R. Pfaendner).

https://doi.org/10.1016/j.polymdegradstab.2026.112080
Received 12 February 2026; Received in revised form 12 March 2026; Accepted 24 March 2026
Available online 30 March 2026
0141-3910/© 2026 The Authors. Published by Elsevier Ltd. This is an open access article under the CC BY license (http://creativecommons.org/licenses/by/4.0/).

and environmental impact of both the stabilizers and their degradation products [8,23–25]. To overcome these limitations, alternative approaches aim to replace conventional phosphites with bio-based and multifunctional stabilizers while maintaining or improving overall stabilization efficiency. Alditols are particularly attractive as sustainable candidates in virgin as well as in recycled grades [26–28]. Their multiple hydroxyl groups provide potential radical scavenging and metal-deactivation properties offering an alternative to conventional phosphites [28–31]. Previous studies have shown strong synergistic effects using α-tocopherol and an alditol mainly attributed to regeneration of the α-tocopheroxyl radical [32,33]. In addition to organic stabilizers, inorganic additives such as calcium oxide or zinc oxide can further enhance the long-term stability of polyolefins [34,35]. The main advantage of inorganic stabilizers are their high thermal stability and their resistance to volatilization as well as to migration [36]. Zinc oxide has gained attention due to its long-term stabilizing and ultraviolet (UV) light protective properties [37–39]. Further, hydrotalcite serves as another highly effective and environmentally friendly acid scavenger [40]. The combined use of these additives in rPP under long-term thermal aging conditions remains largely unexplored and, therefore, warrants in-depth investigation.

The present study investigates the performance of employing different alditols, thiosynergists, and acid scavenger as part of novel stabilizer systems in rPP. In these systems, the conventional phosphite stabilizer is largely replaced by alditols. The effects of the novel stabilizer combinations on surface properties, melt flow behavior, molecular weight, and mechanical properties are systematically evaluated under accelerated aging conditions at different aging temperatures. Fourier-transform infrared spectroscopy was employed to monitor chemical changes during degradation and the carbonyl index was determined as a measure of oxidative damage. The insights gained from this study will help to develop more sustainable and effective stabilizer systems for rPP.

2. Experimental section

2.1. Materials

PP regrind sourced from automotive battery cases (rPP CBC) was provided by Ecobat Resources Braubach GmbH. Calcium stearate (CS) was purchased from Baerlocher GmbH. Pentaerythritol tetrakis(3,5-di-*tert*-butyl-4-hydroxyhydrocinnamate) (Irganox 1010, AO-1) was provided by BASF SE. Tris(2,4-di-*tert*-butylphenyl)phosphite (ADEKA STAB 2112, PS-1) and 2,2-bis{[3-(dodecylthio)-1-oxopropoxy]methyl} propane-1,3-diyl bis[3-(dodecylthio)propionate] (ADK STAB AO-412S, TS-2) were kindly supplied by ADEKA Europe GmbH. RECYCLOBYK 4371 (BYK 4371) was provided by BYK-Chemie GmbH. Bruggolen R8895 (B R8895), erythritol (ALD-1), dioctadecyl 3,3'-thiodipropionate (DSTDP, TS-1), and zinc oxide (AS-1) were provided by L. Brüggemann GmbH & Co. KG. Mannitol (ALD-2) was delivered by VWR GmbH (purity $\geq$ 98.5%). Hydrotalcite (Hycite 713, AS-2, $Mg_6Al_2CO_3(OH)_{16} \cdot 4\ H_2O$) was delivered by Clariant SE. Unless otherwise stated, all chemicals were of industrial grade and all concentrations are given in wt%.

2.2. Accelerated oven aging

Accelerated oven aging to investigate the long-term thermal stability was conducted at 150 °C and 135 °C using a Binder ED115 (Tuttlingen, Germany) oven. The fan power was set at 100%. Both granules and type 5 A tensile test specimens were placed in the oven. The latter were produced on a BABYPLAST 6/10P (Kierspe, Germany) injection molding machine at 200 °C. To promote uniform aging, the granules were stirred and homogenized once per day. Perforated aluminum trays were used to ensure even heat circulation. Samples were taken at predefined intervals for further characterization.

2.3. Material characterization

2.3.1. Tensile testing

The mechanical properties of the samples were evaluated by tensile testing according to DIN EN ISO 527-1. Type 5 A specimens were used for all tests produced on a BABYPLAST 6/10P (Kierspe, Germany) injection molding machine at 200 °C. Measurements were performed on a ZwickRoell Z2.5 (Ulm, Germany) tensile testing machine equipped with a 2.5 kN load cell and a mechanical extensometer. A test speed of 1 mm/min was applied for determination of the tensile modulus, followed by 20 mm/min for measuring tensile strength and elongation at break. A preload of 0.5 N was applied prior to each measurement. All tests were conducted under standard climate conditions according to DIN EN ISO 291 at 23 $\pm$ 2 °C and 50% relative humidity. Five specimens were tested per sample. Average values and standard deviations were calculated from all valid measurements using testXpert III software.

2.3.2. Differential scanning calorimetry

Crystallinities were investigated and determined by differential scanning calorimetry (DSC). DSC measurements were performed in duplicate under nitrogen atmosphere (flow rate: 50 mL/min) on a Mettler Toledo DSC 822e (Columbus, Ohio, USA) device. The standard deviation was calculated based on the average of two independent measurements. DSC specimens were prepared by weighing in 5 to 6 mg sample into a 40 μL standard aluminum crucible. The heating rate was 10 K/min in a temperature range from 25 to 200 °C. The analysis and the determination of the crystallinity was conducted using the STARe software from Mettler Toledo (Columbus, Ohio, USA) with evaluation based on the second heating cycle. The crystallinity (X_c) was calculated from the melting enthalpy (ΔH_m) according to:

$$X_c = \frac{\Delta H_m}{\Delta H_{m,100}} \cdot 100\% \quad (1)$$

To assess the crystallinity percentage of PP, a reference value of 207 J/g [41] was used, representing the melting enthalpy for 100% crystalline PP ($\Delta H_{m,100}$).

Melting points were determined under nitrogen atmosphere (flow rate: 50 mL/min) at a heating rate of 10 K/min over a temperature range in which melting was expected.

2.3.3. Optical microscopy

Optical microscopy images were obtained using an Olympus BX51 (Tokyo, Japan) microscope equipped with an Olympus U-CMAD3 camera adapter. All images were obtained using a plan-fluorite objective (Olympus LMPlanFL N, 10×).

2.3.4. Melt volume rate

The melt volume rate (MVR) was determined according to DIN EN ISO 1133-1 at 230 °C and with 2.16 kg load. Measurements were conducted in duplicate on a Göttfert MI-2 (Buchen, Germany) melt flow rate tester. The dimension of the die was L / D = 8 mm/2.095 mm. For each measurement series, 25 values were recorded and the average was calculated. The standard deviation was then determined based on these averages from both series.

2.3.5. Fourier transform infrared spectroscopy

Fourier transform infrared (FTIR) spectra under attenuated total reflection (ATR) were recorded on a Thermo Nicolet NEXUS 470 (Waltham, Massachusetts, USA) FTIR machine. 32 scans were carried out and the spectral resolution was 4 cm^{-1}. Prior to each recording, a background measurement with the same parameters was performed. A quintuplicate determination was performed. The carbonyl index (CI) was determined from baseline-corrected and integrated band areas (A) using the specified area under band (SAUB) procedure. The integration limits were set from 1850 to 1650 cm^{-1} for the carbonyl band and from

1500 to 1420 cm^{-1} for the reference band corresponding to methylene scissoring [42]. The carbonyl index was calculated according to:

$$CI = \frac{A_{\text{Carbonyl band}}}{A_{\text{Methylene band}}} \quad (2)$$

A linear baseline was taken from data between 4000 and 2000 cm^{-1} and subtracted from the spectra (Fig. S1). The baseline correction, integration, and ratio calculation were performed using a custom Python script applying Simpson's rule for numerical integration. The reported carbonyl index values represent the mean ± standard deviation from quintuplicate determinations.

2.3.6. Gel permeation chromatography

The molecular masses and distributions were determined by high-temperature (HT) gel permeation chromatography (GPC). Analyses were performed using a PolymerChar (Valencia, Spain) GPC-IR, equipped with a 200 μL sample loop, at 160 °C. The mobile phase was 1,2,4-trichlorobenzene (TCB) containing 0.5 g/L butylhydroxytoluene (BHT). The mobile phase flow rate was 1 mL/min. As a stationary phase, three Polymer Standards Service GmbH (PSS, Mainz, Germany) POLEFIN analytical linear XL columns (300 × 8.0 mm, L. × I.D.) with a matching precolumn (50 × 8.0 mm, L. × I.D.) were used. Detection was realized with a fixed wavelength IR detector (IR5, PolymerChar). The data were evaluated using a polystyrene calibration (EasiCal PS-1, Agilent, Waldbronn, Germany) and WinGPC software version 8 from Polymer Standards Service GmbH (Mainz, Germany). For each measurement, approximately 12 mg polymer was automatically mixed with 6 mL mobile phase. Simultaneously, the vials were flushed with nitrogen. Each sample was dissolved under shaking in the autosampler for 1 h at 160 °C before injection. Measurements were conducted in duplicate and the results were averaged and the standard deviations were determined.

2.3.7. Thermogravimetric analysis

Thermogravimetric analysis (TGA) was performed using a Mettler Toledo TGA 2 (Columbus, Ohio, USA) device to determine the decomposition temperature of the additives. Approximately 10 mg of each sample was weighed into a 70 μL aluminum oxide crucible and heated from 35 to 600 °C under nitrogen and air (flow rate: 50 mL/min) at a constant heating rate of 10 K/min.

2.4. Sample preparation

Following the working scheme (Fig. 1), rPP CBC was compounded on a Thermo Haake Rheomex PTW 16 (Waltham, Massachusetts, USA) laboratory twin-screw extruder (Screw diameter: 16 mm, L / D screw ratio: 25). The extrusions were conducted at a throughput of 1.0 kg/h at 200 rpm. The processing was carried out at a temperature profile of 180 °C, 205 °C, 230 °C, 240 °C, and 250 °C from the feed to the nozzle. Prior to extrusion, the additives were premixed with finely ground polymer powder and fed into the extruder via the additive feeder. The remaining material was introduced through the main feeder. Each compound was prepared at a batch size of 1 kg. The formulation codes used are as follows:

STD : Industrial standard formulation.

COM1, COM2 : Commercial state-of-the-art recycling formulations.

F1, F2, F3, F4 : In-house developed formulations.

2.5. Additive formulations

The selection of stabilizer components in this study was guided by their potential to act synergistically under thermo-oxidative conditions relevant for rPP. AO-1 was included as efficient primary antioxidant capable of scavenging peroxy radicals and interrupting the autoxidation cycle. Thiosynergists (TS-1, TS-2) were chosen as classical long-term thermal stabilizers that decompose hydroperoxides and thereby complement phenolic antioxidants through well-established synergistic regeneration pathways [43]. Conventional phosphite stabilizers which are typically used as secondary antioxidants were intentionally replaced by alditols to explore bio-based alternatives [33]. Inorganic acid scavengers (AS-1, AS-2) were incorporated to remove acidic impurities such as catalyst residues or oxidation-derived carboxylic species which are known to accelerate degradation in recycled PP. Based on these considerations, formulation F1 was designed.

Starting from formulation F1 as the reference system with largely replacing conventional phosphite stabilizer by an alditol, individual components were systematically varied relative to F1 to identify synergistic effects between the alditol, thiosynergist, and acid scavenger. Direct comparisons between F2, F3, and F4 are not performed in the discussion. In formulations F2, F3, and F4, the alditol (ALD-1, ALD-2), the type of thiosynergist (TS-1, TS-2), and the metal oxide-based acid scavenger (AS-1, AS-2) were each substituted relative to F1 while maintaining the overall additive concentration. For comparison, a standard formulation (STD) containing conventional antioxidant and phosphite stabilizers as well as two commercially available additive systems (COM1 and COM2) were included. To all formulations, 0.10% CS was added as a processing aid. Table 1 gives an overview of all additive formulations tested in this work.

Concentration variations in F1 and STD as well as samples containing only the processing aid were also studied in accelerated oven aging studies. Mechanical properties, MVR, and CI were measured and are shown in Supporting Information (Fig. S2 to S4).

3. Results and discussion

3.1. Mechanical properties and visual appearance

Basic characterization of rPP CBC was already conducted in previous work of Ng et al. [33]. A polyethylene (PE) content of approximately 10% was determined by ^{13}C nuclear magnetic resonance (NMR) spectroscopy. These foreign polymer fractions may stem from mixing with PE-based waste or from the intentional use of impact-modified PP copolymers in the original PP grades. Furthermore, the oxidation induction time (OIT) and ash content reported in the same study were 6.3 ± 0.4 min (210 °C, synthetic air) and 1.50 ± 0.43% (800 °C, synthetic air), respectively [33]. This suggests only minor amounts of residual phenolic stabilizers and a low filler content in the recycled material. Accelerated oven aging of tensile test specimens (gauge width 3.6 mm, thickness 2.0 mm) was conducted at 150 and 135 °C to evaluate the long-term performance of different stabilizer compositions. Due to the specimen thickness but also the granule dimensions, later used in this study (approximately 3.2 × 1.6 × 2.0 mm^3), diffusion-limited oxidation effects may occur during aging [44]. Under such conditions, the oxygen supply to the polymer bulk becomes limited and causes heterogeneous oxidation. Here, the outer regions of the specimen oxidize faster than the core [45]. As a consequence, gradients in oxidation state and material properties can develop across the specimen thickness.

The time until embrittlement is an industrially relevant parameter and was chosen as a first indicator for material ductility. Here, it is defined as the point at which the elongation at break falls below an absolute value of 50%. It was determined by linear interpolation between the two data points between which the elongation at break crossed the 50% threshold (see Table 2).

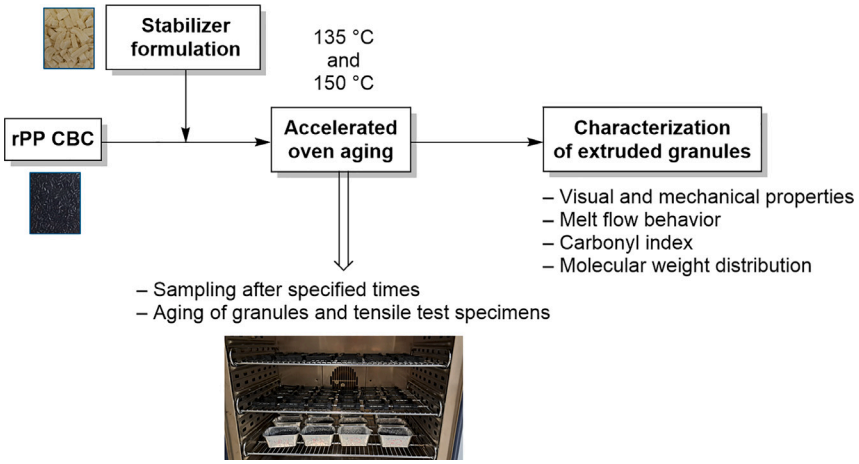

Fig. 1. Representation of the experimental working process of extrusion, oven aging, and analytics.

Table 1
Overview of tested additive formulations, concentrations, and formulation codes used in the multiple extrusion experiments. All formulations contain a total additive concentration of 0.40% and in addition 0.10% CS.

Formulation code	AO-1	PS-1	ALD-1/ALD-2	TS-1/TS-2	AS-1/AS-2	BYK 4371/B R8895
STD	0.200	0.200	–/–	–/–	–/–	–/–
COM1	–	–	–/–	–/–	–/–	0.400/–
COM2	–	–	–/–	–/–	–/–	–/0.400
F1	0.100	0.025	0.075/–	0.100/–	0.100/–	–/–
F2	0.100	0.025	–/0.075	0.100/–	0.100/–	–/–
F3	0.100	0.025	0.075/–	–/0.100	0.100/–	–/–
F4	0.100	0.025	0.075/–	0.100/–	–/0.100	–/–

Table 2
Time until embrittlement (elongation at break < 50%) of rPP CBC at 150 °C and 135 °C are shown using different additive formulations.

Formulation code	Time until embrittlement [h]	
	150 °C	135 °C
Without additional stabilizer	305	1346
STD	713	2054
COM1	438	1622
COM2	724	2227
F1	711	2205
F2	734	2523
F3	734	2447
F4	544	1828

The non-restabilized recyclate embrittled after approximately 300 h at 150 °C and 1350 h at 135 °C indicating limited long-term thermal stability of the rPP CBC despite of some active stabilizer residues. At 150 °C, only moderate differences between the formulations were observed while aging at 135 °C provided a higher resolution of the stabilization efficiency. Among the tested systems F2 containing ALD-2 as an alternative secondary antioxidant exhibited the best performance achieving a time until embrittlement of > 2500 h at 135 °C. Formulation F2 outperforms the commercial reference systems by almost 15% and > 50%, respectively. Also replacing the TS-1 by TS-2 enhances the stabilization performance slightly. However, combinations with AS-2 show an inferior performance compared to AS-1 as acid scavenger. Further important characteristics such as elongation at break and ultimate tensile strength are shown in Fig. 2.

A significant decrease in the elongation at break by more than 50% from the initial state to the first sample withdrawal was observed at both aging temperatures. This can be correlated to an increase in crystallinity or an annealing effect as reported in Kartalis et al. [46]. This effect is more severe in the beginning of the aging process. DSC studies show a crystallinity increase from 33.4 ± 1.9% (unaged) to 38.1 ± 0.3% after 200 h at 150 °C and to 41.2 ± 1.2% after 400 h at 135 °C. At 150 °C, the unstabilized rPP rapidly loses ductility with the elongation at break falling below 50% after around 300 h. All stabilized formulations delay this loss. Differences among them are modest at this temperature. However, most of the formulations extend the ductile regime to above 700 h, whereas F4 fails earlier after around 500 h. The ultimate tensile strength follows a similar trend and stays nearly constant during the early stages of aging and declining only after the material has become brittle. At 135 °C, degradation proceeds more slowly and separates the formulations more clearly. The unstabilized material embrittles after 1200 h, while all stabilized systems exceed 1800 h. F2 performs best reaching > 2500 h before the elongation at break drops below 50% outperforming the commercial references. The ultimate tensile strength at 135 °C exhibits a comparable trend remaining stable for extended periods and decreasing only after embrittlement has occurred. At advanced aging times the specimens reach a degree of brittleness that no tensile deformation was possible anymore resulting in elongation at break and ultimate tensile strength values of zero. The observed differences in the mechanical behavior are also reflected in the visual appearance of the aged specimens. Fig. 3 illustrates the optical changes of the tensile test specimens after oven aging at 135 °C and tensile testing.

The optical appearance of rPP CBC containing F2, which performed best in the tensile tests, was compared with the standard formulations. After 1600 h, all four materials were still intact indicating that mechanical integrity was still maintained. At 2200 h, the sample formulated with STD had already lost mechanical properties completely that it fractured and with formulation COM1 the sample has failed even earlier. At 2400 h, rPP CBC with COM2 showed embrittlement while the material containing F2 remained intact. These visual assessments confirm that F2 provides improved thermo-oxidative aging resistance compared to the standard formulations. To gain further insights into the surface properties, surface microscopic investigations of the aged specimens were performed (Fig. 4). These analyses allow a correlation

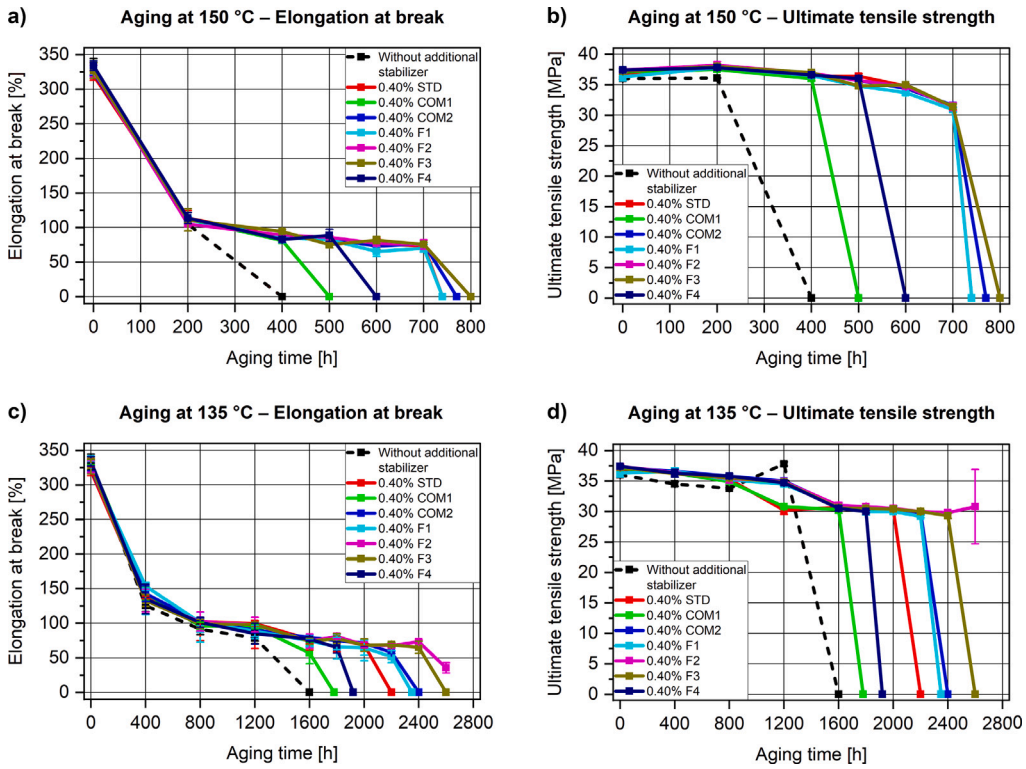

Fig. 2. Elongation at break and ultimate tensile strength of rPP CBC at two different aging temperatures. The elongation at break at (a) 150 °C and (c) 135 °C as well as ultimate tensile strength at (b) 150 °C and (d) 135 °C are shown. Error bars indicate the standard deviation of five measurements. In (a) and (b) between 700 and 800 h, the red curve lies below the light-blue curve, and the pink curve lies below the brown curve, which is why these lines are not visible in this region.

Fig. 3. Appearance of rPP CBC tensile test specimens after oven aging at 135 °C and tensile testing with different stabilizer formulations.

between the macroscopic embrittlement behavior and microstructural changes such as surface crack formation.

The microscopic surface analyses reveal that the sample formulated with STD already exhibits pronounced surface cracking after 2200 h. Additivation with COM2 shows clear and extensive crack formation at 2400 h indicating severe surface degradation. In contrast, the specimens stabilized with F2 display no visible cracks even after 2400 h confirming that the material surface remains largely unaffected despite the prolonged thermal exposure. These findings align well with the macroscopic observations and highlight the superior stabilization efficiency of F2 in suppressing oxidative degradation and delaying crack initiation.

3.2. Aging of granules

The focus was first placed on assessing macroscopic aging effects when investigating the tensile test specimens. In this step, the aging behavior is examined on granules. The analysis of the granules enables the assessment of molecular degradation processes occurring during extrusion without the influence of specimen geometry or molding conditions. For this purpose, measurements of the MVR, the carbonyl index obtained from FTIR spectroscopy, and GPC were conducted to quantify chain scission, oxidation behavior, and changes in molar mass distribution. The evolution of the MVR during accelerated oven aging at 150 °C and 135 °C is shown in Fig. 5.

The increase in MVR with aging time indicates progressive chain scission leading to a reduction in average molecular weight and thus higher flowability. Compared to tensile test specimens, complete failure occurs more rapidly for granules as their smaller size and higher surface-to-volume ratio promote faster oxidative degradation due to increased oxygen accessibility and heat transfer [47]. The unstabilized reference already shows a steep rise in MVR at both temperatures after a comparatively short aging time showing suitable restabilization is necessary when rPP reintroduced into a second life cycle intended for long-term use. At 150 °C, degradation proceeds rapidly and the MVR of the reference material increases sharply after approximately

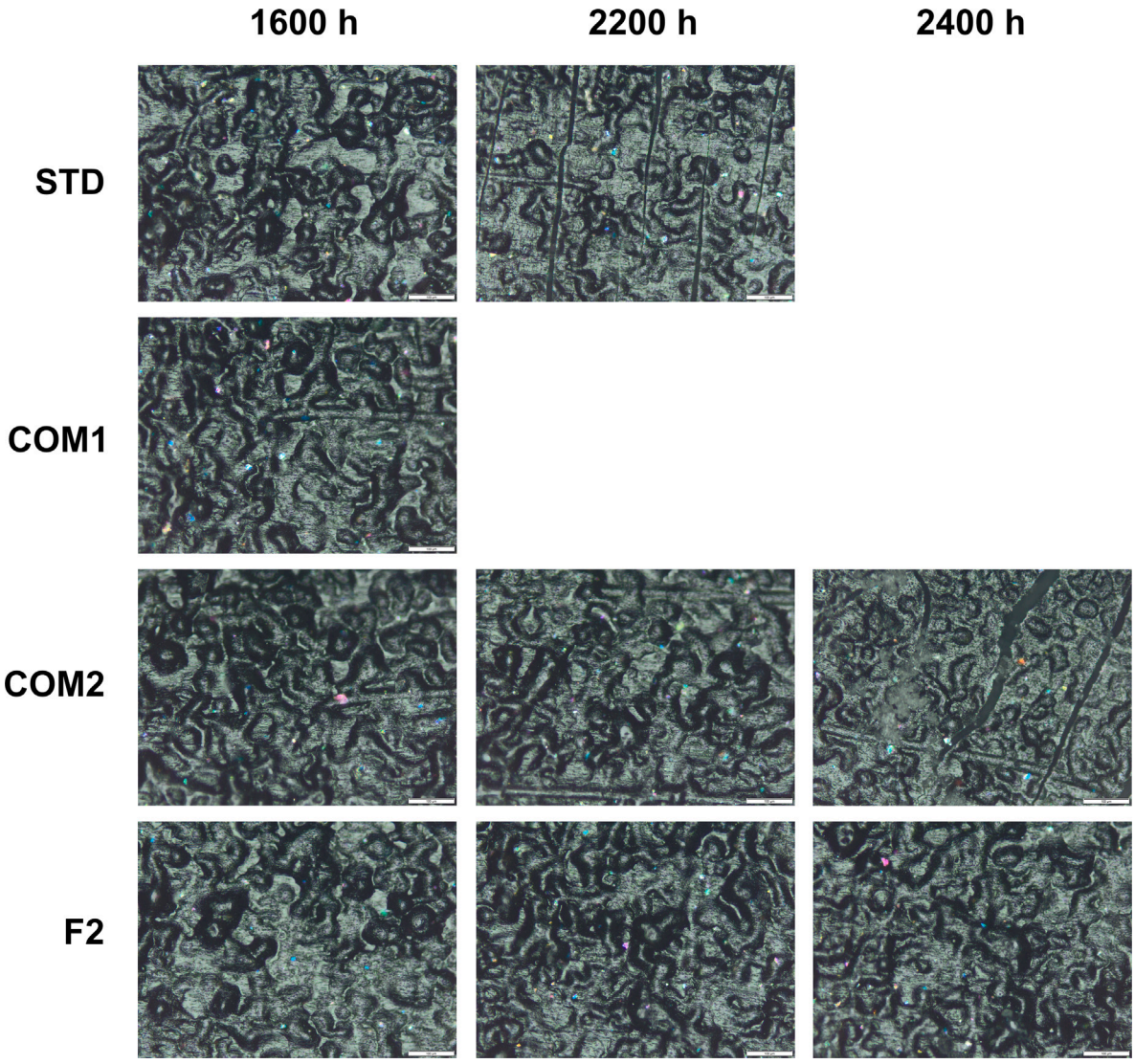

Fig. 4. Surface morphology of oven-aged (135 °C) rPP CBC tensile specimens showing the effect of stabilization on crack formation and surface degradation.

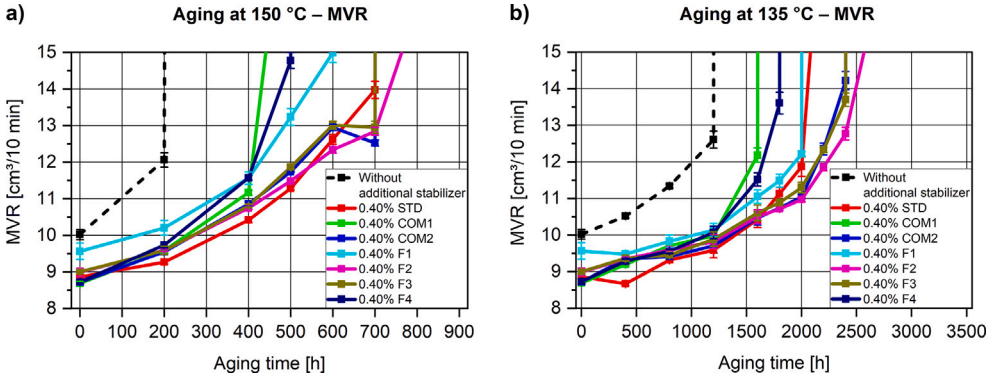

Fig. 5. MVR of rPP CBC at two different aging temperatures with different stabilizer formulations. The MVR of rPP CBC at (a) 150 °C and (b) 135 °C is shown. Error bars indicate the standard deviation of two measurements.

200 h signifying the onset of significant molecular breakdown. As expected, samples containing stabilizers show delayed MVR increase confirming their protective effect. Similar performances were observed for STD, COM2, F2, and F3, all of which maintained MVR values below 13 cm^3/10 min after 600 h of aging indicating effective stabilization against thermal-oxidative aging. At 135 °C, the overall degradation rate is lower as expected due to the reduced temperature. Nevertheless, almost the same trends are observed. It is apparent that STD appears to show slightly inferior stabilization effects at 135 °C aging temperature than at 150 °C compared to other stabilizer systems. However, this observation is likely related to the experimental resolution and scatter of the aging data rather than a mechanistic temperature effect. At both

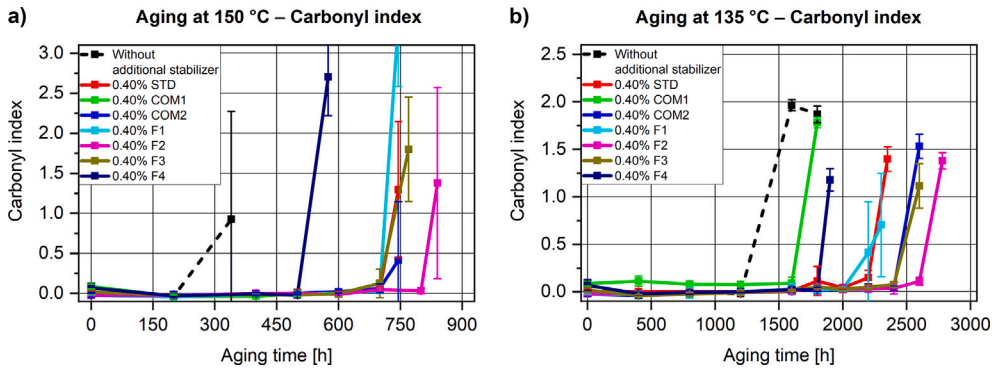

Fig. 6. Carbonyl index of rPP CBC at two different aging temperatures with different stabilizer formulations. The carbonyl index at (a) 150 °C and (b) 135 °C is shown. Error bars indicate the standard deviation of five measurements.

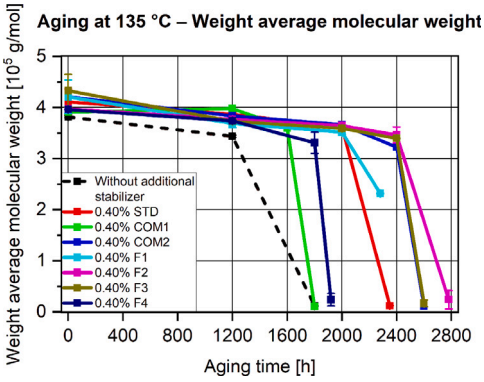

Fig. 7. Evolution of M_w of rPP CBC at 135 °C during accelerated oven aging with different stabilizer formulations. Error bars indicate the standard deviation of two injections.

aging temperatures melt flow properties are best retained by F2. In summary, MVR analysis demonstrates that the addition of bio-based stabilizer combinations can significantly enhance the thermal-oxidative stability of rPP CBC granules during aging. The correlation between MVR increase and molecular degradation will be further discussed in combination with the CI (Fig. 6) monitored via FTIR.

The development of the CI provides complementary information into the progression of oxidative degradation during oven aging of rPP CBC. The sudden rise in carbonyl index is caused by the autocatalytic nature of thermo-oxidative PP degradation where accumulated hydroperoxides decompose rapidly once antioxidants are depleted triggering an exponential formation of carbonyl groups [48]. At 150 °C, the non-restabilized rPP CBC begins to show a pronounced rise already after approximately 300 h indicating the onset of substantial oxidative chain scission reactions. In contrast, all stabilized samples effectively suppress carbonyl formation over an extended period demonstrating their ability to delay oxidative pathways. Formulations COM1 and F4 fail relatively early whereas the other formulations maintain values close to baseline up to about 650 to 750 h which aligns well with the delayed increase in MVR. At 135 °C, the graphs show a similar pathway but shifted to significantly longer induction times. Complementing the MVR and CI data, GPC provides further insights into the molecular structure, particularly the evolution of molecular weight distribution during aging. The number-average molecular weight (M_n), the weight-average molecular weight (M_w) and the dispersity ($Đ$) (Fig. 7 and Tab. S1) were calculated from the molecular weight distribution obtained via GPC.

Fayolle et al. reported for homogeneous PP grades that $Đ$ should tend towards 2 [49] if chain scission is the predominant process. Although this is not the case (Tab. S1), this can be rationalized by the heterogeneous nature of the material after aging due to diffusion limited oxidation effects on the one hand. Furthermore, as an rPP grade, the material consists of a mixture of PP from various sources and also minor amounts of PE. Cross-linking in PP during long-term thermal aging is negligible [50], but minor cross-linking in the PE fraction cannot be excluded [51–53]. Under these conditions, the theoretical convergence by Fayolle et al. for homogeneous polymer systems cannot be expected. Hence, the pronounced and continuous decrease in M_w of the unstabilized reference with aging time indicates thermo-oxidative degradation by chain scission.

This is supported by molecular weight distributions shown in Figure S5. With increasing aging time, the distributions shift towards lower molecular weights and get narrower [49]. At the certain stage a sharp shift occurs. This is characteristic for thermo-oxidative degradation of PP after oxygen uptake, depletion of stabilizers, and the onset of extensive chain scission by autoxidation [54]. The bimodal character of molecular weight distributions after extensive chain scission can be explained by diffusion limited oxidation effects.

The molecular degradation correlates well with the rapid increase in MVR and the steep rise in carbonyl index observed for the reference material. Although the material shows a significantly pronounced rise of the MVR (Fig. 5) with aging time the molecular weights stay relatively close to each other. This is expected, because the melt viscosity and therefore the MVR is highly sensitive to even small changes in molecular weight. In this regime, minor reductions in chain length can already cause disproportionately large increases in flowability consistent with the known scaling behavior of polymer melts (MVR $\sim M_w^{-3.4}$) [55].

All stabilized formulations show a significantly delayed decrease in M_w which demonstrate their effectiveness in suppressing chain scission reactions. Among the investigated systems, formulations COM2, F2, and F3 retain high molecular weight levels for extended aging time consistent with their superior performance in MVR and CI measurements. These findings show the importance of stabilizer selection not only for delaying macroscopic embrittlement but also for preserving the polymer's molecular structure during long-term thermal exposure.

3.3. Mechanistic considerations of alditol stabilization

Alditols used in this study are known to act as stabilizers in polyolefins by multiple mechanisms [8,33]. Beyond their general radical scavenging and regenerative capability, they can also interact with degradation products such as acidic species or acidic catalyst residues [56] (Ziegler–Natta) in the context of short [57] and long-term [58] thermal stabilization or mask metal-ion impurities [59–61]. Fig. 8 illustrates possible mechanisms for the long-term thermal stabilization effects of alditols that have been observed in this study.

The efficacy of acid scavenging mechanisms has been reported in polyvinyl chloride (PVC) systems and provides a mechanistic basis

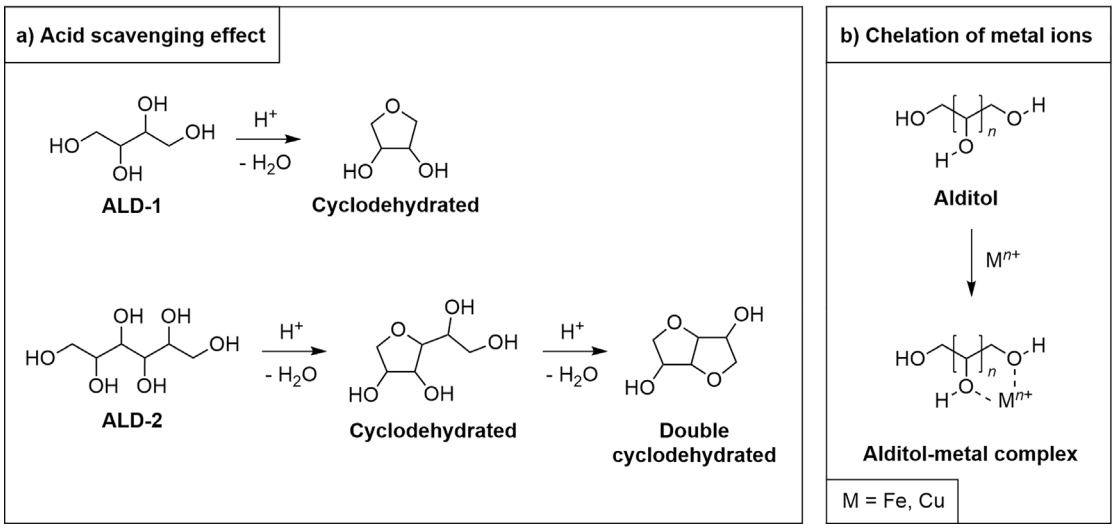

Fig. 8. Schematic illustration of possible long-term thermal stabilization pathways of alditols. (a) Function of alditols as acid scavengers in rPP based on Steenwijk et al. [58] leading to cyclodehydrated products and (b) possible chelation of metal ions that act as pro-oxidants.

Table 3
Thermal properties of investigated additives: Temperature at 10% mass loss determined by TGA under nitrogen and synthetic air, and melting temperature from DSC analysis. Data for ALD-1 and ALD-2 were taken from [33].

Additive	10% mass loss temperature [°C] (Nitrogen/Synthetic air)	Melting temperature [°C] (Nitrogen)
ALD-1	239/239	119
ALD-2	290/275	166
TS-1	346/292	70
TS-2	380/309	53
AS-1	>600/>600	>300
AS-2	222/221	>300

for understanding the observed stabilization in the present formulations [57,58]. It is plausible that this concept can be transferred to polyolefin recyclates, where ALD-1 and ALD-2 may interact with acidic degradation products [62] or acidic impurities [63] and undergo cyclodehydration reactions. In addition, chelation of metal ions by alditols is well known in (aqueous) solvents [29,60] and has also been reported in PE [59]. Here, it can contribute to color inhibition by deactivating catalytically active metal species such as titanium. By suppressing acid-catalyzed reactions and deactivating pro-oxidant metal species, these mechanisms may also reduce the overall oxidation rate and thereby slow the consumption of thiosynergists responsible for hydroperoxide decomposition [56]. A similar, although less pronounced, protective effect may also extend to other antioxidants present in the formulation such as sterically hindered phenolic antioxidants and phosphites [56]. Collectively, these mechanisms provide a reasonable explanation for the improved thermal stability and synergistic performance observed in the formulations investigated in this study.

3.4. Performance and synergies of additive combinations

The performance differences observed among the investigated formulations F1 to F4 can be rationalized by considering synergistic interactions between alditols, thiosynergists, and inorganic acid scavengers and by correlating the analytical results with the thermal properties derived from TGA and DSC analysis (Fig. S6 and S7). Table 3 shows the temperature after 10% mass loss and the melting temperatures of the additives that were varied in this study.

First, possible physical loss of stabilizers during aging should be discussed. During thermal aging, stabilizer depletion may occur either by chemical consumption or by physical loss (e.g., volatilization of low-molecular-weight species) [64]. The stabilizers used in this study exhibit low volatility and high thermal stability. Several of them are high-molecular-weight additives (e.g., sterically hindered phenols, phosphites, and thiosynergists) while the investigated alditols possess very low vapor pressures [65] instead of evaporating at elevated temperatures (Table 3). Therefore, significant loss by volatilization at literature established oven-aging temperatures of 135 and 150 °C is unlikely [64]. Stabilizer depletion is instead expected to occur predominantly through chemical reactions with oxidation products and the possible physical loss of stabilizer degradation products.

Although anisothermal TGA does not directly represent the isothermal aging conditions applied in this study, it provides useful information on the relative thermal stability of the stabilizers. As the onset of mass loss occurs at temperatures far above the aging temperatures, significant stabilizer loss by evaporation is considered unlikely and stabilizer depletion is expected to be dominated by chemical consumption during oxidation. The improved stabilization efficiency of F2 compared to F1 highlights the importance of the alditol selection. ALD-2 exhibits a higher thermal stability than ALD-1 as evidenced by its much higher 10% mass loss temperature in TGA and also a higher molecular weight. This enhanced intrinsic stability allows ALD-2 to remain active over longer aging times and therefore prolongs the induction period against oxidation. The choice of thiosynergist further affects the stabilization performance. Substitution of TS-1 (formulation F1) by TS-2 (formulation F3) results in a modest improvement in long-term performance. This can be attributed to the higher thermal stability and the high molecular weight of TS-2 as indicated by its elevated decomposition temperature in both nitrogen and air atmospheres [66]. A thiosynergist with higher thermal robustness is less prone to thermo-mechanical stress during processing and consumption in early aging stages and hence enables sustained hydroperoxide decomposition. The analytical data support this interpretation as F3 shows delayed increase in MVR and CI as well as delayed decreases in mechanical properties and molecular weight compared to systems with TS-1. In contrast, the replacement of AS-1 with AS-2 in formulation F4 leads to inferior performance despite the generally high thermal stability of hydrotalcite observed in TGA. Notably, AS-2 begins to release water and CO_2 at 220 °C [67,68] which is below the applied processing temperature of 250 °C and may therefore negatively affect its stabilization performance. This interpretation is supported by the TGA graph

shown in Figure S6. Additionally, acid scavengers such as AS-2 have been demonstrated to adsorb small organic substances such as alditols through surface interactions or interlayer incorporation which could also negatively affect long-term stabilization performance [69]. Melting temperatures show that alditols and thiosynergists all melt below the processing temperature promoting homogeneous mixing within the polymer matrix. In contrast, acid scavengers due to their high melting points remain dispersed in the polymer.

4. Conclusions

This work evaluates the effect of a novel and bio-based stabilizer system consisting of different alditols, thiosynergists, and acid scavengers as well as sterically hindered phenol on the long-term stability of a PP recyclate at different temperatures. A systematic variation of the stabilizer component was conducted to elucidate structure-performance relationships and to identify the most effective stabilizer systems. Key findings show that the combination of hexanehexol derivatives, high-molecular-weight thiosynergists, and zinc oxide represents a very effective formulation for stabilizing PP recyclate. Further results show that this formulation significantly outperforms commercial reference systems under long-term thermal aging, particularly at 135 °C by delaying embrittlement, oxidative degradation, and retaining molecular weight. This demonstrates that phosphite-reduced, bio-based stabilizer systems can provide robust long-term thermo-oxidative stability in recycled PP suitable for second-life applications supported by mechanistic considerations. Limitations include that the present work focuses on a single PP recyclate from automotive battery cases while recyclates exhibit different contamination levels, additive histories, or processing damage. Future studies could expand these findings by exploring UV- or light-induced aging and long-term additive migration in processed parts. As a final outlook, the results underline the potential of bio-based and phosphite-reduced (or even phosphite-free) stabilizer concepts to contribute to higher-quality PP recyclate streams. The structure-performance relationships provide a basis for tailoring stabilizer systems to specific recyclate qualities and application requirements. Overall, this work supports the development of more sustainable and durable PP recyclate materials within a circular economy framework.

CRediT authorship contribution statement

Kim Hao Ng: Writing – original draft, Visualization, Methodology, Investigation, Formal analysis, Data curation, Conceptualization. **Katrin Markus:** Writing – review & editing, Methodology, Investigation, Data curation. **Jan-Hendrik Arndt:** Writing – review & editing, Investigation, Formal analysis. **Elke Metzsch-Zilligen:** Supervision, Resources, Project administration. **Rudolf Pfaendner:** Writing – review & editing, Supervision, Conceptualization.

Declaration of competing interest

The authors declare the following financial interests/personal relationships which may be considered as potential competing interests: Rudolf Pfaendner and Elke Metzsch-Zilligen have patents WO2019063550 and WO202319877 issued to Fraunhofer Gesellschaft zur Förderung der Angewandten Forschung e.V. Katrin Markus is involved in plans to establish a start-up company related to the subject of this work. If there are other authors, they declare that they have no known competing financial interests or personal relationships that could have appeared to influence the work reported in this paper.

Acknowledgments

The authors acknowledge financial support from the Federal Ministry of Education and Research (BMBF), Germany, which funded this work under the project “AI Hub Plastic Packaging”. We also express our gratitude to the suppliers of polymers providing us with samples.

Appendix A. Supporting information

Supplementary material related to this article can be found online at https://doi.org/10.1016/j.polymdegradstab.2026.112080.

Data availability

Data will be made available on request.

References

[1] W. Ullah Khan, M. Ahmed Al-Harthi, Research trends in carbon chain polymers and their derivatives: Highlighting the decade-long research, Chem. Rec. 22 (12) (2022) e202200167.
[2] A. Alsabri, F. Tahir, S.G. Al-Ghamdi, Environmental impacts of polypropylene (PP) production and prospects of its recycling in the GCC region, Mater. Today: Proc. 56 (2022) 2245–2251.
[3] S. Bidwai, A. Shivarkar, Polypropylene market revenue 2025 to 2034, 2024, URL: https://www.towardschemandmaterials.com/insights/polypropylene-market. (Accessed: 12 March 2026).
[4] N. Evode, S.A. Qamar, M. Bilal, D. Barceló, H.M.N. Iqbal, Plastic waste and its management strategies for environmental sustainability, Case Stud. Chem. Environ. Eng. 4 (2021) 100142.
[5] A.M. Ragossnig, P. Agamuthu, Plastic waste: Challenges and opportunities, Waste Manag. Res. 39 (5) (2021) 629–630.
[6] European Commission, The European green deal, 2019, URL: https://eur-lex.europa.eu/legal-content/EN/TXT/?uri=CELEX:52019DC0640. (Accessed: 12 March 2026).
[7] T. Gallone, A. Zeni-Guido, Closed-loop polypropylene, an opportunity for the automotive sector, Field Actions Sci. Rep. (2019) 48–53.
[8] R. Pfaendner, Restabilization – 30 years of research for quality improvement of recycled plastics review, Polym. Degrad. Stab. 203 (2022) 110082.
[9] H. Hinsken, S. Moss, J.-R. Pauquet, H. Zweifel, Degradation of polyolefins during melt processing, Polym. Degrad. Stab. 34 (1) (1991) 279–293, Polymer Stabilisation Mechanisms and Applications.
[10] P. Gijsman, Review on the thermo-oxidative degradation of polymers during processing and in service, e-Polymers 8 (1) (2008) 065.
[11] E. Niki, T. Shiono, T. Ido, Y. Kamiya, Oxidative degradation of polyolefins. I. Thermal oxidative degradation of atactic polypropylene in solution, J. Appl. Polym. Sci. 19 (12) (1975) 3341–3353.
[12] J. Lacoste, D. Vaillant, D.J. Carlsson, Gamma-, photo-, and thermally-initiated oxidation of isotactic polypropylene, J. Polym. Sci. Part A: Polym. Chem. 31 (3) (1993) 715–722.
[13] P. Gijsman, J. Hennekens, J. Vincent, The mechanism of the low-temperature oxidation of polypropylene, Polym. Degrad. Stab. 42 (1) (1993) 95–105.
[14] G. Grause, M.-F. Chien, C. Inoue, Changes during the weathering of polyolefins, Polym. Degrad. Stab. 181 (2020) 109364.
[15] J. Pospíšil, Z. Horák, Z. Kruliš, S. Nešpůrek, The origin and role of structural inhomogeneities and impurities in material recycling of plastics, Macromol. Symp. 135 (1) (1998) 247–263.
[16] P. Gijsman, R. Fiorio, Long term thermo-oxidative degradation and stabilization of polypropylene (PP) and the implications for its recyclability, Polym. Degrad. Stab. 208 (2023) 110260.
[17] J. Pospíšil, F.A. Sitek, R. Pfaendner, Upgrading of recycled plastics by restabilization—an overview, Polym. Degrad. Stab. 48 (3) (1995) 351–358.
[18] R. Pfaendner, H. Herbst, K. Hoffmann, F. Sitek, Recycling and restabilization of polymers for high quality applications. An overview, Die Angew. Makromol. Chem. 232 (1) (1995) 193–227.
[19] N.S. Allen, A.P. Jones, C.M. Liauw, M. Edge, K. Keck-Antoine, J.-H. Yeo, High-temperature stabilization of polypropylene using hindered phenol–thioester stabilizer combinations, part 1: Optimization and efficacy via nondust blends, J. Vinyl Addit. Technol. 27 (2) (2021) 376–388.
[20] C. Armstrong, M.J. Husbands, G. Scott, Mechanisms of antioxidant action: Antioxidant-active products formed from the dialkyl thiodipropionate esters, Eur. Polym. J. 15 (3) (1979) 241–248.
[21] K. Schwetlick, W.D. Habicher, Organophosphorus antioxidants action mechanisms and new trends, Die Angew. Makromol. Chem. 232 (1) (1995) 239–246.
[22] J. Pospíšil, Mechanistic action of phenolic antioxidants in polymers—A review, Polym. Degrad. Stab. 20 (3) (1988) 181–202.
[23] R. Liu, S.A. Mabury, Synthetic phenolic antioxidants: A review of environmental occurrence, fate, human exposure, and toxicity, Environ. Sci. Technol. 54 (19) (2020) 11706–11719.
[24] X. Li, N. Zhao, J. Fu, Y. Liu, W. Zhang, S. Dong, P. Wang, X. Su, J. Fu, Organophosphate diesters (Di-OPEs) play a critical role in understanding global organophosphate esters (OPEs) in fishmeal, Environ. Sci. Technol. 54 (19) (2020) 12130–12141.

[25] S. Ai, X. Chen, Y. Zhou, Critical review on organophosphate esters in water environment: Occurrence, health hazards and removal technologies, Environ. Pollut. 343 (2024) 123218.
[26] E. Metzsch-Zilligen, R. Pfaendner, Method for stabilizing halogen-free thermoplastic recyclates, stabilized plastic compositions, and molding compounds and molded parts produced therefrom, 2019, Fraunhofer-Gesellschaft zur Förderung der angewandten Forschung e.V., WO2019063550.
[27] E. Metzsch-Zilligen, R. Pfaendner, Method of stabilizing virgin thermoplastic material and stabilized plastic compositions, moulding compounds and mouldings produced therefrom, stabilizers compositions and uses thereof, 2020, Fraunhofer-Gesellschaft zur Förderung der angewandten Forschung e.V., WO2020083740.
[28] H. Aschenbach, M. Ahle, E. Metzsch-Zilligen, R. Pfaendner, Stabilised, transition-metal-containing plastics compositions, moulding compound or moulded part and use of a stabiliser composition for stabilising transition-metal-containing plastics, 2023, Fraunhofer-Gesellschaft zur Förderung der angewandten Forschung e.V., WO2023198777.
[29] L. Yang, W. Tian, Y. Xu, Y. Su, S. Gao, Z. Wang, S. Weng, C. Yan, J. Wu, Interactions between metal ions and carbohydrates: the coordination behavior of neutral erythritol to transition metal ions, J. Inorg. Biochem. 98 (8) (2004) 1284–1292.
[30] G.J.M. den Hartog, A.W. Boots, A. Adam-Perrot, F. Brouns, I.W.C.M. Verkooijen, A.R. Weseler, G.R.M.M. Haenen, A. Bast, Erythritol is a sweet antioxidant, Nutrition 26 (4) (2010) 449–458.
[31] R. Pfaendner, A brief history of plastic additives. Part 1: Antioxidants, Macromol. Mater. Eng. 310 (8) (2025) 2500039.
[32] R.-T. Lan, Y. Ren, X. Wei, L.-Z. Tang, N.A. Shah, L. Xu, S.-S. Huang, R.M. Gul, J.-Z. Xu, Z.-M. Li, Synergy between vitamin E and D-sorbitol in enhancing oxidation stability of highly crosslinked ultrahigh molecular weight polyethylene, Acta Biomater. 134 (2021) 302–312.
[33] K.H. Ng, J.-H. Arndt, E. Metzsch-Zilligen, R. Pfaendner, Processing stabilization of polyolefin recyclates using alditols in combination with α-tocopherol: A sustainable alternative to phosphites, J. Vinyl Addit. Technol. (2026).
[34] K. Hoffmann, H. Herbst, R. Pfaendner, H.-J. Sander, F. Sitek, Process for the stabilization of a stabilizer mixtures for recycled plastic mixtures, 2003, Ciba Specialty Chemicals Corporation, US6525158.
[35] A. Plota-Pietrzak, A. Masek, Functionalized metal oxide particles with antioxidant as new carriers providing higher stability of polyolefin products, Sustain. Mater. Technol. 40 (2024) e00885.
[36] T. Zaharescu, A.B. Lugao, Stability improvement of irradiated polymer composites by inorganic compounds—A pertinent solution with respect to phenolic antioxidants, J. Compos. Sci. 9 (1) (2025) 47.
[37] A. Ammala, A.J. Hill, P. Meakin, S.J. Pas, T.W. Turney, Degradation studies of polyolefins incorporating transparent nanoparticulate zinc oxide UV stabilizers, J. Nanoparticle Res. 4 (2002) 167–174.
[38] N. Miyatake, H.-J. Sue, L. Yuntao, Y. Yamaguchi, Stabilization of polymers with zinc oxide nanoparticles, 2006, Kaneka Corp Texas and A&M University System. US20060194910.
[39] D. Rasouli, N.T. Dintcheva, M. Faezipour, F.P. La Mantia, M.R. Mastri Farahani, M. Tajvidi, Effect of nano zinc oxide as UV stabilizer on the weathering performance of wood-polyethylene composite, Polym. Degrad. Stab. 133 (2016) 85–91.
[40] G. Zhao, F. Wang, J. Feng, Effect of hydrotalcite on the thermal stabilization performance of natural antioxidant vitamin E in Ziegler-Natta polyethylene, Polym. Degrad. Stab. 241 (2025) 111534.
[41] D.R. Gee, T.P. Melia, Thermal properties of melt and solution crystallized isotactic polypropylene, Die Makromol. Chem. 132 (1) (1970) 195–201.
[42] J. Almond, P. Sugumaar, M.N. Wenzel, G. Hill, C. Wallis, Determination of the carbonyl index of polyethylene and polypropylene using specified area under band methodology with ATR-FTIR spectroscopy, E-Polymers 20 (1) (2020) 369–381.
[43] S. Beer, I. Teasdale, O. Brueggemann, Macromolecular antioxidants via thiol-ene polyaddition and their synergistic effects, Polym. Degrad. Stab. 110 (2014) 336–343.
[44] C.R. Boss, J.C.W. Chien, Oxygen diffusion limitation in autoxidation of polypropylene, J. Polym. Sci. Part A-1: Polym. Chem. 4 (6) (1966) 1543–1551.
[45] K. Grabmayer, S. Beißmann, G.M. Wallner, D. Nitsche, K. Schnetzinger, W. Buchberger, H. Schobermayr, R.W. Lang, Characterization of the influence of specimen thickness on the aging behavior of a polypropylene based model compound, Polym. Degrad. Stab. 111 (2015) 185–193.
[46] C.N. Kartalis, C.D. Papaspyrides, R. Pfaendner, K. Hoffmann, H. Herbst, Recycled and restabilized hdpe bottle crates: Retention of critical properties after heat aging, Polym. Eng. Sci. 41 (5) (2001) 771–781.
[47] D.L. Faulkner, Aging of polypropylene using high oxygen pressure: Influence of sample thickness and stabilization, J. Appl. Polym. Sci. 31 (7) (1986) 2129–2138.
[48] J. Verdu, On the autoaccelerated character of the branched oxidation of polyolefins, Macromol. Symp. 115 (1) (1997) 165–180.
[49] B. Fayolle, E. Richaud, J. Verdu, F. Farcas, Embrittlement of polypropylene fibre during thermal oxidation, J. Mater. Sci. 43 (3) (2008) 1026–1032.
[50] S. Luzuriaga, J. Kovářová, I. Fortelný, Degradation of pre-aged polymers exposed to simulated recycling: Properties and thermal stability, Polym. Degrad. Stab. 91 (6) (2006) 1226–1232.
[51] F.P. La Mantia, A. Valenza, D. Acierno, Thermomechanical degradation of blends of isotactic polypropylene and high density polyethylene, Polym. Degrad. Stab. 13 (1) (1985) 1–9.
[52] J. Pospíšil, Z. Horák, Z. Kruliš, S. Nešpurek, S. ichi Kuroda, Degradation and aging of polymer blends I. Thermomechanical and thermal degradation, Polym. Degrad. Stab. 65 (3) (1999) 405–414.
[53] Y. Shangguan, C. Zhang, Y. Xie, R. Chen, L. Jin, Q. Zheng, Study on degradation and crosslinking of impact polypropylene copolymer by dynamic rheological measurement, Polymer 51 (2) (2010) 500–506.
[54] H.J.O. ad E. Turi, The deterioration of polypropylene by oxidative degradation, Polym. Eng. Sci. 5 (3) (1965) 152–158.
[55] M. Doi, Explanation for the 3.4-power law for viscosity of polymeric liquids on the basis of the tube model, J. Polym. Sci.: Polym. Phys. Ed. 21 (5) (1983) 667–684.
[56] N.S. Allen, M. Edge, Perspectives on additives for polymers. 1. Aspects of stabilization, J. Vinyl Addit. Technol. 27 (1) (2021) 5–27.
[57] J. Steenwijk, D.S. van Es, J. van Haveren, J.W. Geus, L.W. Jenneskens, The effect of (natural) polyols on the initial colour of heavy metal- and zinc-free poly(vinyl chloride), Polym. Degrad. Stab. 91 (9) (2006) 2233–2240.
[58] J. Steenwijk, R. Langerock, D.S. van Es, J. van Haveren, J.W. Geus, L.W. Jenneskens, Long-term heat stabilisation by (natural) polyols in heavy metal- and zinc-free poly(vinyl chloride), Polym. Degrad. Stab. 91 (1) (2006) 52–59.
[59] N.S. Allen, C.M. Liauw, A. Reyes, M. Edge, B. Johnson, K. Keck-Antoine, Color inhibition of phenolic antioxidants in Ziegler-Natta polyethylene. I. In-situ polymer studies, J. Vinyl Addit. Technol. 15 (1) (2009) 12–19.
[60] N.S. Allen, C.M. Liauw, A. Reyes, M. Edge, B. Johnson, K. Keck-Antoine, Color inhibition of phenolic antioxidants in Ziegler-Natta polyethylene. II. In-situ solution studies, J. Vinyl Addit. Technol. 15 (4) (2009) 234–243.
[61] M.A. Al-Mamary, Z. Moussa, Antioxidant activity: The presence and impact of hydroxyl groups in small molecules of natural and synthetic origin, in: V. Waisundara (Ed.), Antioxidants - Benefits, Sources, Mechanisms of Action, IntechOpen, London, 2021.
[62] A. Jansson, K. Möller, T. Gevert, Degradation of post-consumer polypropylene materials exposed to simulated recycling—mechanical properties, Polym. Degrad. Stab. 82 (1) (2003) 37–46.
[63] G.N. Foster, S.H. Wasserman, D.J. Yacka, Oxidation behavior and stabilization of metallocene and other polyolefins, Die Angew. Makromol. Chem. 252 (1) (1997) 11–32.
[64] J. Pospíšil, Z. Horák, J. Pilař, N.C. Billingham, H. Zweifel, S. Nešpurek, Influence of testing conditions on the performance and durability of polymer stabilisers in thermal oxidation, Polym. Degrad. Stab. 82 (2) (2003) 145–162.
[65] W. Yan, G.J. Suppes, Vapor pressures and evaporation studies of sugars and sugar alcohols, J. Chem. Eng. Data 53 (9) (2008) 2033–2040.
[66] Q. Liu, D. Peng, P. Wei, H. Song, C. Cong, X. Meng, Q. Zhou, Synthesis of macromolecular antioxidants containing thioether and aromatic secondary amine to improve the anti-oxidation properties of EPDM, Polym. Degrad. Stab. 218 (2023) 110585.
[67] L. Pesic, S. Salipurovic, V. Markovic, D. Vucelic, W. Kagunya, W. Jones, Thermal characteristics of a synthetic hydrotalcite-like material, J. Mater. Chem. 2 (1992) 1069–1073.
[68] J. Pérez-Ramírez, G. Mul, F. Kapteijn, J.A. Moulijn, Investigation of the thermal decomposition of Co–Al hydrotalcite in different atmospheres, J. Mater. Chem. 11 (2001) 821–830.
[69] J. Orthman, H.Y. Zhu, G.Q. Lu, Use of anion clay hydrotalcite to remove coloured organics from aqueous solutions, Sep. Purif. Technol. 31 (1) (2003) 53–59.